IEEE Access
Multidisciplinary | Rapid Review | Open Access Journal

Received 9 December 2023, accepted 26 December 2023, date of publication 1 January 2024, date of current version 22 January 2024.

Digital Object Identifier 10.1109/ACCESS.2023.3348169

RESEARCH ARTICLE

Robust State Estimation Method Based on Mahalanobis Distance Under Non-Gauss Noise

HUANQIANG ZHANG[1], QUAN XU[2], YI XIE[1], XINHAO LIN[2], RUIRONG DING[1], YINLIANG LIU[2], CANSHU QIU[1], AND PENG CHEN[1]

[1]Chaozhou Power Supply Bureau of Guangdong Power Grid Company Ltd., Chaozhou, Guangdong 521000, China
[2]CSG Electric Power Research Institute Company Ltd., Guangzhou, Guangdong 510663, China

Corresponding author: Huanqiang Zhang (584618721@qq.com)

ABSTRACT Under non-Gauss noise condition, the performance of traditional state estimation methods based on Gauss measurement noise will be greatly reduced. In order to solve this problem, a robust state estimation method based on Mahalanobis distance under non-Gauss noise is proposed in this paper. First of all, based on the Mahalanobis distance, the calculation method of optimal buffer length for PMU measurements is used, which can unify the SCADA measurements with PMU measurements in the same snapshot. Then, Based on the two-stage processing method, in the first stage, the SCADA measurements are used for filtering by using maximum likelihood estimator to obtain the estimated values, and then the estimated values in the first-stage are combined with PMU measurements as the second-stage measurements for filtering, and finally the final results are obtained. Based on the IEEE-39 buses system and IEEE-118 buses system, under Gaussian noise and non-Gaussian noise, the AEE results of proposed method are very small, and which are all within 10^{-3}, numerical tests under different simulation conditions verified the robustness and effectiveness.

INDEX TERMS Non-Gauss noise, optimal buffer length, two-stage, maximum likelihood estimator, state estimation.

I. INTRODUCTION

The purpose of state estimation (SE) is to obtain the voltage result that is closest to the true value of the network when given the network topology and parameters [1]. Therefore, the accuracy of estimation results is influenced by measurement errors and estimation models [2]. However, due to the measurement error of the measuring device, all measurements are affected and inevitably have errors [3]. Seriously, the measurements may have large error which is called bad data in SE [5], [6]. Moreover, due to the changes of operating environment, network parameters may also change, thus exhibiting the uncertainty of the SE model [4]. Therefore, the noise of measurement errors in practice is unknown and may not necessarily be strictly Gaussian noise [5], [6].

The associate editor coordinating the review of this manuscript and approving it for publication was Akshay Kumar Saha.

Nowadays, phasor measurement units (PMU) are widely deployed in power system [7], but it can not completely replace the traditional supervisory control and data acquisition system (SCADA) for the time being [10]. The data collected by PMU and SCADA will coexist in power system for a long time [8]. In the field of SE, how to combine SCADA data and PMU data fully and effectively to maximize the estimation performance is an important focus of current research [9], [10].

Therefore, the combination of PMU data and SCADA data for mixed data filtering has been paid more and more attention [11], [12]. Based on the mixed data processing method, literature [13] directly mixes PMU data and SCADA data for estimation. This method is direct, simple and easy to implement, but it also has the following three disadvantages: (1) First of all, it needs to modify the key parts of the program, such as Jacobian matrix, which makes its program is not extensible [14]; (2) Secondly, when doing SE in each snapshot, the PMU data and SCADA data are mixed to construct a measurement equation for filtering processing, which will cause the PMU data and SCADA data to interact with each other, so that the PMU data with higher measurement accuracy will be polluted by the SCADA data with lower measurement accuracy [15]; (3) Thirdly, the sampling frequency of PMU is not synchronous with SCADA data, which has the problem of data delay [16]. Therefore, it is necessary to unify the two types of data under the same snapshot when combining them [17].

The method to deal with bad data can be divided into two main types, namely methods for looking for bad data in SCADA measurements and methods for looking for bad data with multiple data sources such as PMU [18]. The former method focuses on the use of Lagrange multiplier, hypothesis tests, or robust estimators for analyzing residuals. In recent years, with the increase of PMU deployed in the transmission network, the use of PMU measurement has attracted great attention in the detection of bad key measurements [19].

Furthermore, most of the current researches assume that the measurement noise obeys Gaussian distribution [20]. However, in practice, the noise of measurement errors is unknown and may not necessarily be strictly Gaussian noise, which may be characterized as heavy tail noise, and is called non-Gaussian noise in this paper. Under non-Gaussian noise, the performance of traditional SE methods based on Gaussian measurement noise will degrade significantly. At the same time, as the sampling frequency of PMU and SCADA is different, the two types of data need to be unified under the same snapshot.

Therefore, a robust state estimation method based on mahalanobis distance under non-Gauss noise is proposed in this paper. The main contributions in this paper are as follow:

(1) A two-stage state estimation method is proposed. Based on the two-stage processing method, in the first stage, the SCADA measurements are used for filtering to obtain the first-stage estimated values, and then the first-stage estimated values and PMU measurements are combined as the second-stage measurement for filtering, and then the final results are obtained. The proposed method can effectively avoid the interaction between PMU and SCADA data compared with the mixed data processing method in one stage.

(2) The maximum likelihood estimator is used in the two-stage state estimation, which can limit the influence of bad data and estimated residuals, and produce good estimation results for Gauss noise or non-Gauss heavy-tail distribution noise (such as Laplacian, Gauss mixed and other non-Gauss noise).

(3) The calculation method of optimal buffer length for PMU is used based on Mahalanobis distance, which can unify PMU and SCADA data in the same snapshot when combining them.

II. NON-GAUSSIAN DISTRIBUTED NOISE AND THE OPTIMAL BUFFER LENGTH CALCULATION METHOD

A. EQUATION FOR MEASURING NON-GAUSSIAN DISTRIBUTED NOISE

In practice, we can not know the noise statistics measured by SCADA or PMU, and the noise of measurement errors is unknown and may not necessarily be strictly Gaussian noise. In this paper, the measurement noise is represented by the following ε-pollution model (i.e., non-Gaussian noise model):

$$G(e) = (1-\varepsilon)\Phi(e) + \varepsilon K(e) \tag{1}$$

where $\Phi(e)$ represents Gaussian distribution; $K(e)$ represents unknown distribution, which is called heavy-tailed distribution, such as Laplace distribution and Gaussian distribution with large variance; ε represents contamination coefficient, which is used to adjust the contribution of non-Gaussian distribution; $G(e)$ represents non-Gaussian distribution.

For non-Gaussian noise model (1), by adjusting the contamination coefficient ε, non-Gaussian distribution can be obtained as follow:

-When $\varepsilon = 0$, it is pure Gaussian distribution noise;

-When $0 < \varepsilon < 1$, it is non-Gaussian distribution noise;

-When $\varepsilon = 1$, it is pure unknown distribution, such as Laplace distribution.

Then, the measurement-state equation in the power system can be formulated as follow:

$$z = h(x) + G(e) \tag{2}$$

where z represents the measurement; $h(x)$ represents the measurement function; x represents the state quantity.

B. THE OPTIMAL BUFFER LENGTH CALCULATION METHOD BASED ON THE MAHALANOBIS DISTANCE

As the sampling frequency of PMU is not synchronous with SCADA data, so it is necessary to unify the two types of data under the same snapshot when combining them [17]. In this paper, the calculation method of optimal buffer length for PMU is used based on Mahalanobis distance [21], [22]. All PMU measurement points are treated as a whole, so that the buffer length of each PMU measurement point is the same.

The sampling frequency of the PMU is $n_r = 30$ samples/second. The sampling frequency of the SCADA measurements is $N_t = 5$ seconds. In this paper, we assume that the SE is updated every 5 seconds. During two SCADA sampling intervals, the PMU sampling sequence are $N = N_t * n_r = 150$PMU samples. The measurement matrix is Z, and divide Z into $n_{subset} = N_t = 5$ subsets, the number of measurements in each subset is $n_{meas} = 30$. Then, the measurement matrix Z is represented by $n_{subset} = 5$ subsets as: $Z = [Y_1, Y_2, Y_3, Y_4, Y_5]_,$. Y_1, Y_2, Y_3, Y_4, Y_5 represent $n_{subset} = 5$ subsets of Z.

The calculation steps to determine the optimal buffer length for all PMU points are as follows:

(1) Obtain the median value of the matrix Z, which can be formulated as follow:

$$Y' = median(Z) = \left[y'_1, y'_2, y'_3, y'_4, y'_5\right] \tag{3}$$

where: Y' represent the median value of the matrix Z; *median* represent the function to get the median value; $y'_1, y'_2, y'_3, y'_4, y'_5$ represent the median value of Y_1, Y_2, Y_3, Y_4, Y_5.

(2) Change point detection is performed on the latest measurement subset Y_5, and if a change occurs, there will be no PMU buffer and the latest received PMU data, i.e. sample 150 is accepted. Otherwise, Y_5 will be included in the PMU buffer length and proceed to the third step;

(3) Based on Mahalanobis distance, the following matrix $\eta_1 = [y'_5, y'_4]$, $\eta_2 = [y'_4, y'_3]$,..., $\eta_4 = [y'_2, y'_1]$ are used to detect system changes. The formula for calculating the robust Mahalanobis distance is:

$$P_i = \max\left(\frac{\left|y_i^T v - median(y_j^T v)\right|}{\lambda \cdot median\left(\left|y_i^T v - median(y_j^T v)\right|\right)}\right), \quad \|v\| = 1 \tag{4}$$

where T represent the transposition operation; P_i represent the Mahalanobis distance; λ represent the correction factor. If P_i is less than $\varsigma_1 = \chi^2_{2,0.975}$, then Y_4 will be included in the PMU buffer length and continue to detect $\eta_2 = [y'_4, y'_3]$, ..., $\eta_4 = [y'_2, y'_1]$. Eventually, we can get the PMU buffer set Z'.

(4) For the optimal PMU buffer set Z', the statistical mean $\bar{h}$ and variance $\bar{C}$ of measurements can be calculated:

$$\bar{h} = \frac{\sum_{i=1}^{\alpha} w_i h_i}{\sum_{i=1}^{\alpha} w_i} \tag{5}$$

$$\bar{C} = \frac{\sum_{i=1}^{\alpha} (w_i h_i - \bar{h})(w_i h_i - \bar{h})^T}{\sum_{i=1}^{\alpha} w_i - 1} \tag{6}$$

where α is the number of columns of the PMU buffer set Z', w_i is the weight of the i-th column of Z', and $w_i = \min(1, \varsigma_2/P_i^2)$, $\varsigma_2 = \chi^2_{\alpha,0.975}$.

After the above calculation steps, the optimal buffer length of PMU measurement points can be calculated, and the statistical mean $\bar{h}$ and variance $\bar{C}$ of measurements for PMU buffer can be obtained, which is unified with SCADA data in the same snapshot.

III. TWO-STAGE ROBUST STATE ESTIMATION METHOD BASED ON MAHALANOBIS DISTANCE

The method proposed in this paper consists of two stages:

(1) Robust nonlinear SE with using SCADA data, called the first stage SE;

(2) Robust linear SE with using PMU data and estimated results from the first stage, called the second stage.

A. FIRST-STAGE MAXIMUM LIKELIHOOD ESTIMATION BASED ON SCADA MEASUREMENTS

In robust nonlinear SE based on SCADA measurements, the maximum likelihood estimator is used to deal with non-Gaussian measurement noise or bad data. The goal is to minimize the following function J:

$$J = \sum_{i=1}^{m} w_i^2 \rho(r_{si}) \tag{7}$$

where: w_i^2 represent the weight, $w_i = \min(1, d^2/PS_i^2)$, $d = 1.5$; m represent the number of SCADA measurements; PS_i is a projection statistic; $\rho(r_{si})$ is a nonlinear convex function, which can be formulated as follow:

$$\rho(r_{si}) = \begin{cases} \frac{1}{2} r_{s_i}^2, & \left|r_{s_i}\right| < c \\ c\left|r_{s_i}\right| - \frac{c^2}{2}, & else \end{cases} \tag{8}$$

where $r_{s_i} = r_i/sw_i$ represent the standardized residual; s represents robust parameter; $r_i = z_i - h_i(x)$ represents the residual; c represent the constant.

The robust parameter s can be calculated as follows:

$$s = 1.1926 f_m \bullet \underset{i=1,\ldots,m}{lomed} \; \underset{j \neq i}{lomed} \left|r_i - r_j\right| \tag{9}$$

where f_m represents the factor; the external operator *lomed* represents the low median (i.e., the $[(m+1)/2]$ order statistic in the m-th numbers), for example, in number series "1,2,3,4,5,6", 3 is the low median value; the internal operator *lomed* represents the high median(i.e., the $[m/2]+1$ order statistic in the m-th numbers), for example, in number series "1,2,3,4,5,6", 4 is the high median value; [ ] represents the integer operator.

In order to minimize the objective function (7), yields the partial derivative of (7):

$$\frac{\partial J}{\partial x} = \sum_{i=1}^{m} -\frac{w_i a_i}{s_i^2} \psi(rs_i) = 0 \tag{10}$$

where $\Psi(rs_i) = \partial\rho(rs_i)/\partial\rho rs_i$; a_i represents the i-th row element of Jacobian matric $H = \partial h/\partial x$.

The equation (10) is multiplied and divided by the standardized residual simultaneously, yields:

$$\sum_{i=1}^{m} -\frac{w_i a_i}{s_i^2} \frac{\psi(r_{s_i})}{r_{s_i}} r_{s_i} = 0 \tag{11}$$

Then, the following matrix form can be obtained:

$$H^T Q R^{-1}(z - h(x)) = 0 \tag{12}$$

where $Q = diag(q(r_{s_i}))$, $q(r_{s_i}) = \Psi(r_{s_i})/r_{s_i}$ and $R = diag(s_i^2)$; *diag* represent the diagonal operation.

Newton iteration method is used for (12), and the state correction equation for the k-th iteration is:

$$(H^T Q_k R^{-1} H)\Delta x_k = H^T Q_k R^{-1}(z - h(x_k)) \tag{13}$$

The convergence condition is:

$$\|\Delta x_k\|_\infty = \|x_{k+1} - x_k\|_\infty \leq 10^{-3} \tag{14}$$

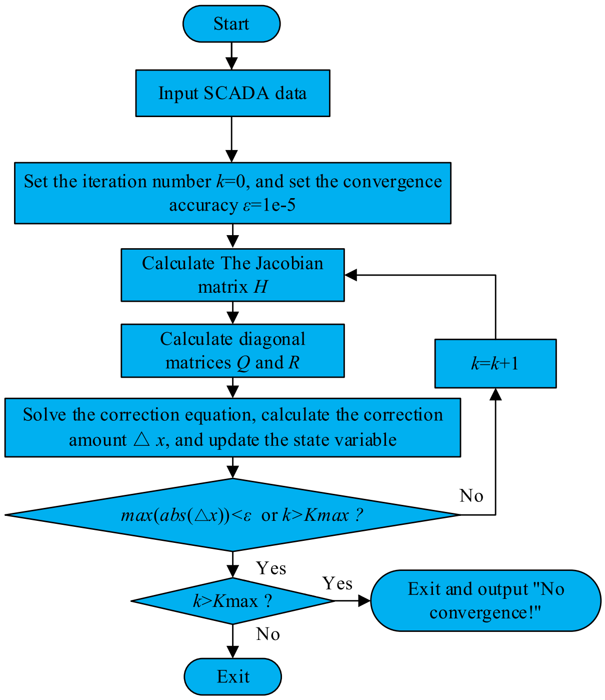

FIGURE 1. **The first stage calculation flowchart based on SCADA measurements.**

To improve numerical robustness, using the Givens rotation, the equivalent form of the reconstructed state correction equation is:

$$\underbrace{(Q_k^{1/2}R^{-1/2}H)}_{\tilde{H}}\,\Delta x_k = \underbrace{Q_k^{1/2}R^{-1/2}(z-h(x_k))}_{\tilde{Z}} \tag{15}$$

where $\tilde{H}$ represents corrected Jacobian matric in first stage; $\tilde{z}$ represents corrected measurements in first stage.

The covariance matrix Σ of the maximum likelihood state estimator is [22]:

$$\Sigma = \frac{E_\Phi\left[\Psi^2(r_s)\right]}{\{E_\Phi\left[\Psi'(r_s)\right]\}^2}(H^TH)^{-1}(H^TQ_wH)(H^TH)^{-1} \tag{16}$$

where E_Φ represent the probability distribution of r; $Q_w = diag(w_i^2)$.

The first stage of robust SE based on SCADA measurements is calculated as follows:

(1) Initialize the state quantity x, set the convergence threshold ε, the maximum iterations K max and the number k=0 of current iteration;

(2) calculate the Jacobian matrix H;

(3) calculate the diagonal matrices Q and R;

(4) Calculate the increment of state quantity Δx_k;

(5) If max $|\Delta x_k| < \varepsilon$, the algorithm converges, otherwise, go to step (6);

(6) $x_{k+1} = x_k + \Delta x_k$, $k = k + 1$, go to step (2).

The calculation flowchart for the first stage SE is shown in Figure 1.

B. SECOND-STAGE MAXIMAL LIKELIHOOD ESTIMATION BASED ON PMU MEASUREMENTS

The PMU configured on the bus can measure the voltage phasor and branch current phasor. In the second stage SE, PMU measurements are combined with the estimated results from the first stage as the second stage measurements, and the measurement equation is as follow:

$$Z = Ax + \varepsilon \tag{17}$$

where $Z = \begin{bmatrix} x_s & z_p \end{bmatrix}^T$ represent measurement vector in the second stage, including PMU measurements z_p and the estimated results from the first stage x_s; $A = \begin{bmatrix} I & M \end{bmatrix}^T$ represents the correlation between measurements Z and state variable x, I represents identity matrix, M represents the constant matrix, it is a linear correlation between PMU measurements and state variables; $\varepsilon = \begin{bmatrix} e_s & e_p \end{bmatrix}^T$ represents the error vector of Z, whose covariance matrix $P = E\left[\varepsilon\varepsilon^T\right] = SS^T, R_P = diag(\sigma_{p1}^2, \ldots, \sigma_{pN}^2)$, e_s and e_p represents the error vector of x_s and z_p; S can be calculated by the Cholesky decomposition.

Multiply S^{-1} in both sides of equation (17), we can get:

$$y = Gx + \xi \tag{18}$$

where $y = S^{-1}Z$ represent the corrected measurements; $G = S^{-1}A$ represent the Jacobian matric in the second stage; ξ represents the error vector of y, $E\left[\xi\xi^T\right] = I$.

Similar to the first-stage maximum likelihood estimation solution, establishing the objective function and minimizing it, yields:

$$G^T\tilde{Q}(y - Gx) = 0 \tag{19}$$

where $\tilde{Q}$ can be calculated as Q in the first stage. Using Newton iteration method for (19), the state correction equation for the j-th iteration is:

$$\underbrace{Q_j^{1/2}G}_{\hat{H}}\,\Delta x_j = \underbrace{Q_j^{1/2}y}_{\hat{Z}} \tag{20}$$

where $\hat{H}$ represents corrected Jacobian matric in second stage; $\hat{z}$ represents corrected measurements in second stage.

The calculation process of the first stage and the second stage is basically the same. The comparisons between the first stage filtering and the second stage filtering are as follows:

(1) The use of measurement is different. In the first stage, SCADA measurement is used, and in the second stage, the estimation result of the first stage and PMU measurement are combined as the second stage measurement.

(2) The measurement equation is different. The first stage measurement includes nonlinear measurement such as power, and the measurement equation is nonlinear. In the second stage, all measurements are linear measurements such as voltage phasor and current phasor, and the measurement equation is linear equation.

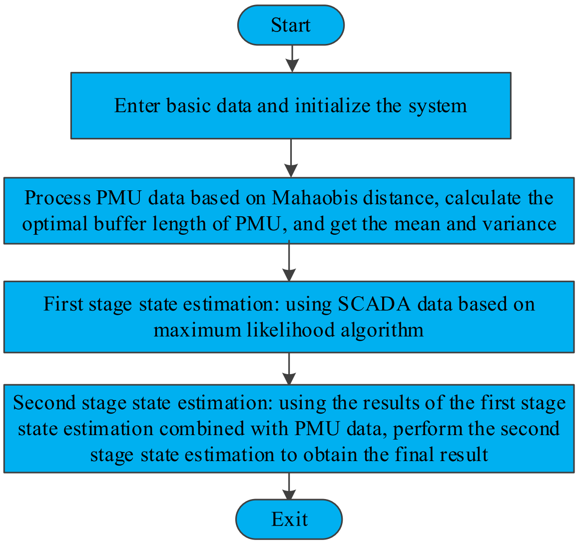

FIGURE 2. The flowchart of robust SE method based on Mahalanobis distance.

C. THE STEPS OF TWO-STAGE ROBUST STATE ESTIMATION

Under non-Gaussian noise, the steps for calculating the two-stage maximal likelihood robust SE based on Mahalostobis distance are as follows:

(1) Enter the basic data, initialize the state quantity x, set the convergence threshold;

(2) Calculate the optimal PMU buffer length and obtain the statistical mean $\bar{h}$ and variance $\bar{C}$ of the PMU buffer;

(3) First-stage SE based on maximum likelihood algorithm using SCADA data;

(4) Combining the first-stage SE results with PMU data to carry out the second-stage SE to obtain the final results.

The calculation steps of the two-stage maximum likelihood robust SE method based on Mahalanobis distance are shown in Figure 2.

IV. NUMERICAL TEST AND ANALYSIS

A. SIMULATION DATA

Based on the IEEE-39 buses system, numerical tests under different simulation conditions are conducted to verify the robustness and effectiveness of the proposed method. The structure of the IEEE-39 buses system is shown in Figure 3. In IEEE 39 buses system, there are 39 buses, 10 generators and 46 branches. All the measurements are obtained on the MATLAB simulation platform based on IEEE 39 buses standard system.

The measurement configuration of the system is: SCADA measurements are fully configured based on the results of traditional power flow calculation, which is assumed true value in the system. The corresponding error is added in the true value as the measurement. Eight PMU measurement points are deployed on buses 7, 11, 13, 22, 27, 28, 30 and 32 to increase the measurement redundancy. The PMU can measure the bus voltage phasor and branch current phasor, including their amplitude and phase angle. No. 31 bus is used as the phase reference point, and the parameters in this paper are set to $c = d = 1.5$.

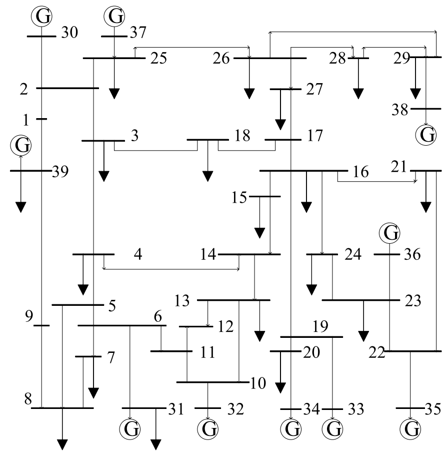

FIGURE 3. IEEE-39 buses system structure diagram

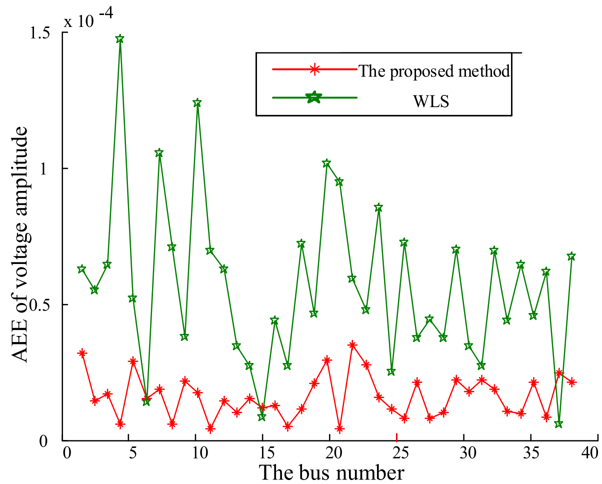

FIGURE 4. The AEE of the voltage amplitude under Gaussian noise.

A two-stage weight least square (WLS) non-robust estimator is used to compare with the method proposed herein, and the absolute estimation error (AEE) is used to evaluate the estimation accuracy. AEE is defined as follow:

$$AEE = |x_{estimated} - x_{ture}| \tag{21}$$

where $x_{estimated}$ represents estimated value; x_{ture} represents true value.

B. SIMULATION RESULTS AND ANALYSIS

(1) Simulation results under Gaussian noise

Under Gaussian noise, ε=0, for SCADA and PMU measurement, measurement error is assumed 1.5% and 0.15% Gaussian noise, respectively. In this case, the AEE of the two-stage WLS and the method proposed herein are shown in Figure 4 and Figure 5.

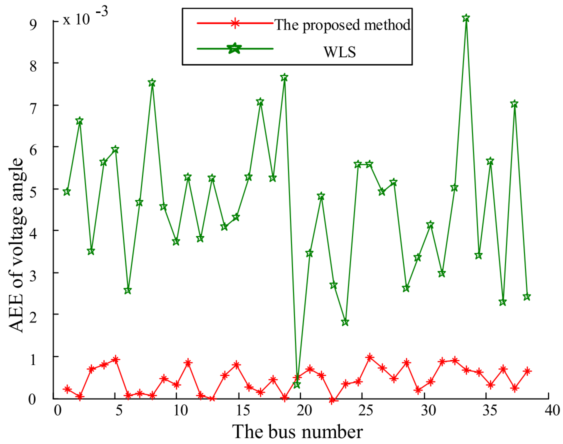

FIGURE 5. The AEE of the voltage angle under Gaussian noise.

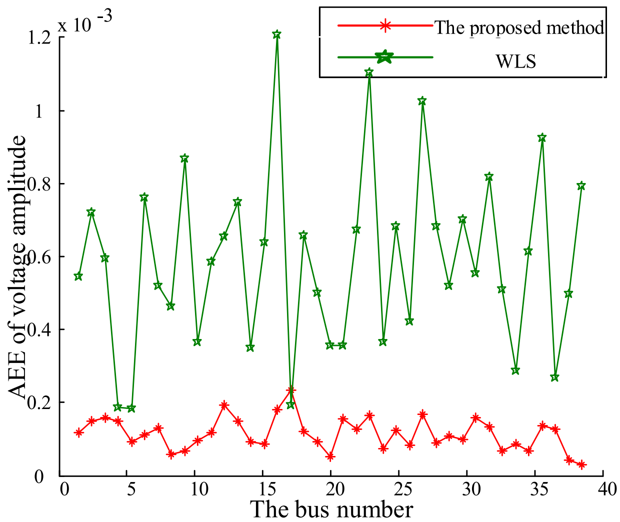

FIGURE 6. The AEE of the voltage amplitude under first type of Gaussian noise.

From Figure 4 and Figure 5, it can be found that the AEE results of the two-stage WLS non-robust estimator and the proposed method in this paper are all very small. Furthermore, under Gaussian noise, most of the results estimated by the proposed method are much better than the WLS. The AEE of voltage amplitude in WLS are all within 10^{-4}, and the AEE of voltage amplitude in the proposed method are all within 10^{-5}, therefore, the proposed method has better estimation performance than WLS.

(2) Simulation results under non-Gaussian noise

Under non-Gaussian noise, two types are considered:

-Use the ε-pollution model with ε=0.12. For SCADA and PMU, whose variance is assumed 10^{-4} and 10^{-6} respectively to represent Gaussian noise $\Phi(e)$. For $K(e)$, 100 times variance of $\Phi(e)$ is used for SCADA and PMU;

-Use the ε-pollution model with ε=1. Noise for SCADA and PMU measurements error using Laplace distribution, whose mean is zero and scale parameter is set at 1.2.

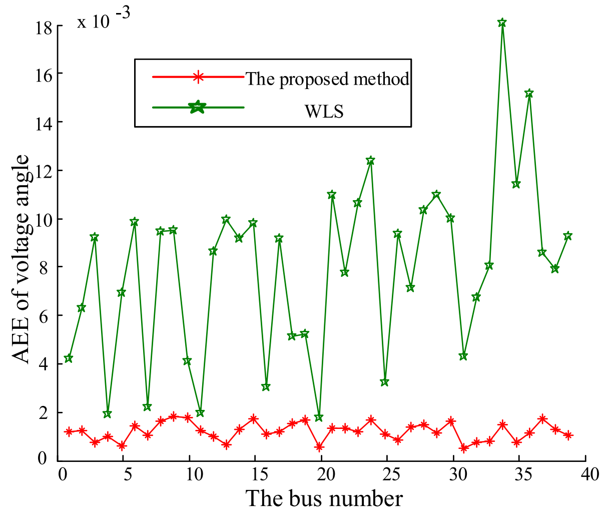

FIGURE 7. The AEE of the voltage angle under first type of Gaussian noise.

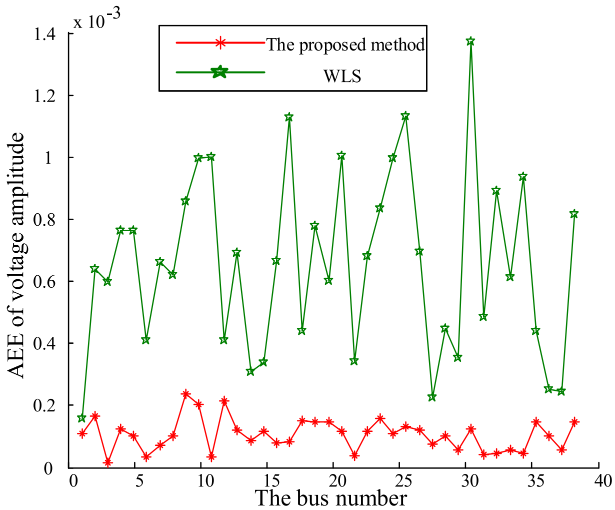

FIGURE 8. The AEE of the voltage amplitude under the second type of Gaussian noise.

Under the first and second non-Gaussian noise, the AEE results of the two-stage WLS and the method proposed in this paper are shown in Figure 6 and Figure 7, Figure 8 and Figure 9.

From the results of Figure 6 to Figure 9, and comparing them with Figure 4 and Figure 5, it can be found that the estimated AEE of the two-stage WLS estimator in Figure 6 to Figure 9 is much higher under non-Gaussian noise and Laplace noise, compared to the estimated AEE obtained in Figure 4 and Figure 5 under the assumption of Gaussian measurement noise. Furthermore, in Figure 6 and Figure 8, the AEE of voltage amplitude estimated by WLS are all within 10^{-3}, and the AEE of voltage amplitude estimated by the proposed method are all within 10^{-4}. And seen from Figure 9, the AEE of voltage angle estimated by WLS are larger than the proposed method. Obviously, the proposed robust estimator herein can effectively constrain the influence

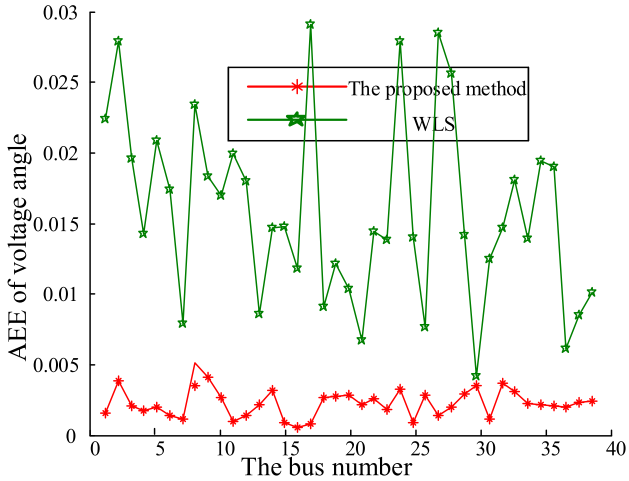

FIGURE 9. The AEE of the voltage angle under the second type of Gaussian noise.

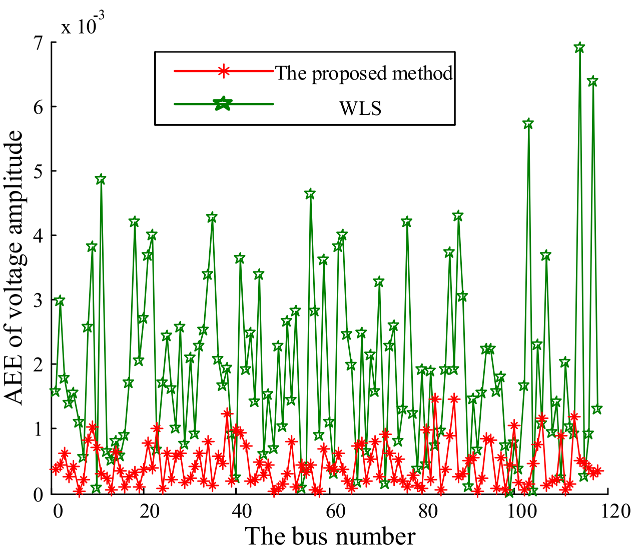

FIGURE 10. The AEE of the voltage amplitude in IEEE 118 buses system.

of heavy thick-tail distribution, not only the results are significantly better (the AEE results are all smaller than WLS), but also the method itself can maintain good estimation statistical efficiency under Gaussian or non-Gaussian noise environment.

In order to prove the effectiveness of the proposed method in other IEEE standard networks, further simulation is carried on IEEE 118 buses system. Simulation conditions are consistent with "the ε-pollution model with ε=1". The AEE results of the two-stage WLS and the method proposed in this paper are shown in Figure 10 and Figure 11.

From Figure 10 and Figure 11, it can be seen that the AEE of the proposed method in this paper are still smaller than WLS. The results are basically consistent with those of IEEE 39 buses system, which shows that the proposed method is still effective in other IEEE standard networks as well.

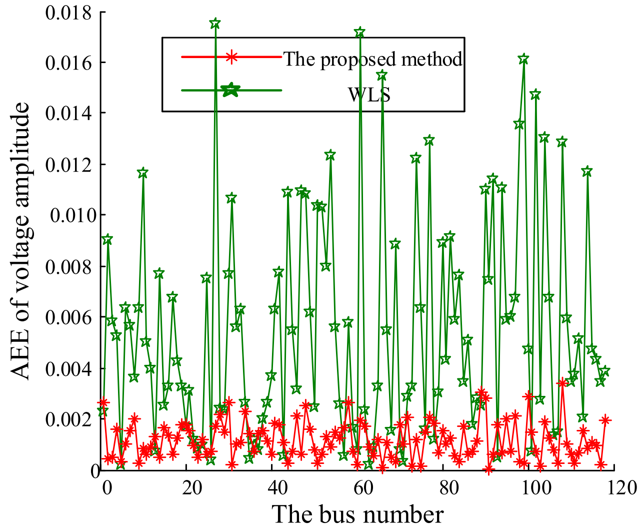

FIGURE 11. The AEE of the voltage angle in IEEE 118 buses system.

V. CONCLUSION

In this paper, a robust SE method combining SCADA and PMU measurements under non-Gaussian noise is proposed.

(1) By using the Mahalanobis distance, the optimal PMU buffer length for PMU measurement is calculated, which can unify the SCADA measurements with PMU measurements in the same snapshot.

(2) The proposed robust two-stage SE method can effectively avoid the interaction between PMU and SCADA data compared with the mixed data processing method in one stage.

(3) By using the maximum likelihood estimator, the proposed method can effectively limit the influence of unknown heavy-tailed non-Gaussian noise and meanwhile maintain good robustness.

Under Gaussian noise and non-Gaussian noise, the AEE results of proposed method are all very small, and which are all within 10^{-3}. Numerical tests under different simulation conditions verified the robustness and effectiveness.

In the follow-up research, the research on the defense of false data attack in power system and the research on the detection and identification of false data combined with cyber-physical systems model will be carried in the future.

REFERENCES

[1] H. Long, Z. Wu, C. Fang, W. Gu, X. Wei, and H. Zhan, "Cyber-attack detection strategy based on distribution system state estimation," *J. Modern Power Syst. Clean Energy*, vol. 8, no. 4, pp. 669–678, Jul. 2020.

[2] F. Feng, P. Zhang, and Y. Zhou, "Authentic microgrid state estimation," *IEEE Trans. Power Syst.*, vol. 37, no. 2, pp. 1657–1660, Mar. 2022.

[3] Y. Wang, M. Xia, Q. Yang, Y. Song, Q. Chen, and Y. Chen, "Augmented state estimation of line parameters in active power distribution systems with phasor measurement units," *IEEE Trans. Power Del.*, vol. 37, no. 5, pp. 3835–3845, Oct. 2022.

[4] P. Shen, M. Ouyang, L. Lu, J. Li, and X. Feng, "The co-estimation of state of charge, state of health, and state of function for lithium-ion batteries in electric vehicles," *IEEE Trans. Veh. Technol.*, vol. 67, no. 1, pp. 92–103, Jan. 2018.

[5] B. Jiang, H. Dai, and X. Wei, "A cell-to-pack state estimation extension method based on a multilayer difference model for series-connected battery packs," *IEEE Trans. Transport. Electrific.*, vol. 8, no. 2, pp. 2037–2049, Jun. 2022.
[6] Y. Gao, K. Liu, C. Zhu, X. Zhang, and D. Zhang, "Co-estimation of state-of-charge and state-of-health for lithium-ion batteries using an enhanced electrochemical model," *IEEE Trans. Ind. Electron.*, vol. 69, no. 3, pp. 2684–2696, Mar. 2022.
[7] J. Zhao, M. Netto, Z. Huang, S. S. Yu, A. Gómez-Expósito, S. Wang, I. Kamwa, S. Akhlaghi, L. Mili, V. Terzija, A. P. S. Meliopoulos, B. Pal, A. K. SinghA. Abur, T. Bi, and A. Rouhani, "Roles of dynamic state estimation in power system modeling, monitoring and operation," *IEEE Trans. Power Syst.*, vol. 36, no. 3, pp. 2462–2472, May 2021.
[8] P. V. Patil, L. Vachhani, S. Ravitharan, and S. Chauhan, "Sequential state and unknown parameter estimation strategy and its application to a sensor fusion problem," *IEEE Sensors J.*, vol. 22, no. 21, pp. 20665–20675, Nov. 2022.
[9] Y. Chen, H. Chen, Y. Jiao, J. Ma, and Y. Lin, "Data-driven robust state estimation through off-line learning and on-line matching," *J. Modern Power Syst. Clean Energy*, vol. 9, no. 4, pp. 897–909, Jul. 2021.
[10] R. Gao, F. Tronarp, and S. Särkkä, "Variable splitting methods for constrained state estimation in partially observed Markov processes," *IEEE Signal Process. Lett.*, vol. 27, pp. 1305–1309, 2020.
[11] G. Tian, Y. Gu, D. Shi, J. Fu, Z. Yu, and Q. Zhou, "Neural-network-based power system state estimation with extended observability," *J. Modern Power Syst. Clean Energy*, vol. 9, no. 5, pp. 1043–1053, Sep. 2021.
[12] H. Liu, P. Wang, J. Lin, H. Ding, H. Chen, and F. Xu, "Real-time longitudinal and lateral state estimation of preceding vehicle based on moving horizon estimation," *IEEE Trans. Veh. Technol.*, vol. 70, no. 9, pp. 8755–8768, Sep. 2021.
[13] G. Tan and Z. Wang, "Generalized dissipativity state estimation of delayed static neural networks based on a proportional-integral estimator with exponential gain term," *IEEE Trans. Circuits Syst. II, Exp. Briefs*, vol. 68, no. 1, pp. 356–360, Jan. 2021.
[14] J. Kim, J.-H. Kang, J. Bae, W. Lee, and K. K. Kim, "Distributed moving horizon estimation via operator splitting for automated robust power system state estimation," *IEEE Access*, vol. 9, pp. 90428–90440, 2021.
[15] L. Li and X. Song, "State estimation for systems with packet dropping and state equality constraints," *IEEE Trans. Circuits Syst. II, Exp. Briefs*, vol. 66, no. 9, pp. 1572–1576, Sep. 2019.
[16] J. Zhao, G. Zhang, Z. Y. Dong, and M. La Scala, "Robust forecasting aided power system state estimation considering state correlations," *IEEE Trans. Smart Grid*, vol. 9, no. 4, pp. 2658–2666, Jul. 2018.
[17] W. Zhang, L. Wang, L. Wang, C. Liao, and Y. Zhang, "Joint state-of-charge and state-of-available-power estimation based on the online parameter identification of lithium-ion battery model," *IEEE Trans. Ind. Electron.*, vol. 69, no. 4, pp. 3677–3688, Apr. 2022.
[18] S. Ghorbani and F. Janabi-Sharifi, "Extended Kalman filter state estimation for aerial continuum manipulation systems," *IEEE Sensors Lett.*, vol. 6, no. 8, pp. 1–4, Aug. 2022.
[19] J. Li, L. Ma, S. Feng, X. Shi, and F. Song, "Three phase linear state estimation method of substation based on zero impedance model," *IEEE Access*, vol. 11, pp. 29380–29390, 2023.
[20] X. Wang, Y. Liu, Z. Li, and S. Sun, "Enhanced maximum exponential square state estimator based on simulation-hyperparameter optimization," *IEEE Trans. Power Syst.*, vol. 38, no. 6, pp. 5957–5960, Nov. 2023.
[21] Z. Chang, W. Chen, Y. Gu, and H. Xu, "Mahalanobis–Taguchi system for symbolic interval data based on kernel Mahalanobis distance," *IEEE Access*, vol. 8, pp. 20428–20438, 2020.
[22] D. D. N. Nguyen, K. Sood, M. R. Nosouhi, Y. Xiang, L. Gao, and L. Chi, "RF fingerprinting-based IoT node authentication using Mahalanobis distance correlation theory," *IEEE Netw. Lett.*, vol. 4, no. 2, pp. 78–81, Jun. 2022.

HUANQIANG ZHANG is currently an Engineer with Chaozhou Power Supply Bureau of Guangdong Power Grid Company Ltd. His research interests include power system control and protection and power system state estimation.

QUAN XU is currently an Engineer with CSG Electric Power Research Institute Company Ltd. His research interests include power system control and protection and optimal dispatch of power systems.

YI XIE is currently an Engineer with Chaozhou Power Supply Bureau of Guangdong Power Grid Company Ltd. His research interests include power system control and protection, power system state estimation, and power system transient analysis.

XINHAO LIN is currently an Engineer with CSG Electric Power Research Institute Company Ltd. His research interests include power system control and protection and optimal dispatch of power systems.

RUIRONG DING is currently an Engineer with Chaozhou Power Supply Bureau of Guangdong Power Grid Company Ltd. His research interests include power system control and protection and power system state estimation.

YINLIANG LIU is currently an Engineer with CSG Electric Power Research Institute Company Ltd. His research interests include power system control and protection and optimal dispatch of power systems.

CANSHU QIU is currently an Engineer with Chaozhou Power Supply Bureau of Guangdong Power Grid Company Ltd. His research interests include power system control and protection and power system state estimation.

PENG CHEN is currently an Engineer with Chaozhou Power Supply Bureau of Guangdong Power Grid Company Ltd. His research interests include power system control and protection and energy system optimization and scheduling.